Nuclear Medicine and Biology 146-147 (2025) 109032

Contents lists available at ScienceDirect

Nuclear Medicine and Biology

journal homepage: www.elsevier.com/locate/nucmedbio

Preclinical evaluation of [^{225}Ac]Ac-PSMA-617 and *in vivo* effect comparison in combination with [^{177}Lu]Lu-PSMA-617 for prostate cancer☆

E. Savio *, L. Reyes, J. Giglio, L. Alfaya, G. Falasco, L. Urrutia, M. Bentura, K. Zirbesegger, F. Arredondo, P. Duarte, J.P. Gambini, R. Dapueto

I&D Biomédico y Químico Farmacéutico, Departamento de Radiofarmacia, Centro Uruguayo de Imagenología Molecular, Montevideo, Uruguay

ARTICLE INFO

Keywords:
Prostate cancer
Targeted alpha therapy
Actinium-225
Lutetium-177, [^{225}Ac]Ac PSMA-617, LNCaP PC3

ABSTRACT

Introduction: The interest in targeted alpha therapy (TAT) has grown in the recent years as it can provide new treatment options for advanced- and late-stage cancer. In this sense, the use of actinium-225 is rising showing promising results. Even more, combining alpha and beta (lutetium-177) radionuclides might help to minimize actinium adverse effects, while preserving treatment efficacy. Preclinical studies of actinium-225-PSMA-targeting tracers for advanced prostate cancer and the "cocktail" combination with lutetium-177-PSMA needs to be further explored.

Methods: In vitro properties of [^{225}Ac]Ac-PSMA-617 using the human prostatic cancer cell lines, LNCaP (PSMA+) and PC3 (PSMA-) were investigated by means of antiproliferative, binding, cytotoxicity and clonogenic studies. *In vivo* de-escalated treatment protocols of actinium-225/lutetium-177-PSMA-617 "cocktail"-regimens were also assessed in order to improve the tolerability of ^{225}Ac-PSMA-617 TAT. A four-branch study with ([^{177}Lu]Lu-PSMA-617 and [^{225}Ac]Ac-PSMA-617) or its combination was successfully performed in a xenographic nude mice model bearing prostate cancer. Tumour growth was monitored by external caliper measurements and PET-CT imaging with [^{18}F]F-AlF-PSMA-11 over two months.

Results: Specific dose-dependent inhibition proliferation of [^{225}Ac]Ac-PSMA-617 was observed in LNCaP cells (IC_{50} = 0.14 KBq/mL) whereas an antiproliferative effect in PC3 cells required an activity concentration two orders of magnitude higher (IC_{50} = 15.5 KBq/mL). In autoradiography binding studies, [^{225}Ac]Ac-PSMA-617 had significant higher affinity for LNCaP cells, compared to PC3 cells, which probed to be specific under blocking conditions. Cytotoxicity assay evidenced a 200-fold higher toxicity in LNCaP cells. The percentage of colony survival significantly decreased in LNCaP cells treated with 1 KBq/mL and 10 KBq/mL, as compared to PC3 cells treated with the same activity concentrations. The co-administration of both beta and alpha therapeutical radiopharmaceuticals to xenographic nude mice model bearing prostate cancer showed the best results in terms of survival, growth rates and absence of tumour at the endpoint of the study.

Conclusion: This study shows that PSMA radioisotope therapy (RIT) and TAT combined therapy could improve patient management by delaying disease progression.

1. Introduction

Prostate cancer (PCa) is one of the most common types of cancer in men, being the second most diagnosed cancer and the fifth leading cause of cancer death among men worldwide [1]. Prostate-specific membrane antigen (PSMA) is a membrane-bound protein overexpressed in 90 % of PCa patients and therefore has become a major target in the treatment of advanced prostate cancer [2,3].

Radionuclide therapy using the small molecule PSMA bound to the beta-emitting radionuclide, Lutetium-177 ([^{177}Lu]Lu-PSMA-617) is a suitable line of therapy, having demonstrated efficacy and survival benefit in patients bearing castrate resistant metastatic disease who have already been treated with androgen receptor (AR) pathway inhibition and taxane-based chemotherapy [4–6]. The phase 3 VISION trial (NCT03511664) evaluated the efficacy and safety of the radioligand [^{177}Lu]Lu-PSMA-617 in patients with metastatic castration-resistant

☆ This article is part of a Special issue entitled: 'Targeted Alpha Therapy' published in Nuclear Medicine and Biology.

* Corresponding author.
E-mail address: eduardo.savio@cudim.org (E. Savio).

https://doi.org/10.1016/j.nucmedbio.2025.109032
Received 2 February 2025; Received in revised form 9 May 2025; Accepted 28 May 2025
Available online 6 June 2025

prostate cancer (CRPC). [^{177}Lu]Lu-PSMA-617 plus protocol-permitted standard of care (SOC) significantly improved overall survival and radiographic progression-free survival of patients compared with SOC alone [7]. Although CRPC patients treated with [^{177}Lu]Lu-PSMA-617 experience increased survival and reduced PSA blood levels, enhancing therapeutic efficacy remains essential [8].

Targeted alpha therapy (TAT) provides new treatment options for advanced- and late-stage cancer diseases [3]. Alpha particles have a higher linear energy transfer (LET) and a shorter tissue range ($\leq$ 100 μm), causing higher probability of DNA double strand breaks (DSB) with a reduced chance of damaging surrounding healthy cells, compared to beta particles [9,10]. Actinium-225 is an alpha-emitting radionuclide considered particularly promising for TAT because of its favourable half-life (9.92 days) and its emission of four α-particles in the decay cascade.

In preclinical research, alpha-radiation demonstrated stronger induction of abscopal effects than beta-radiation; favoring its usage as a combination partner with immunotherapies [11]. Thus, further evaluation of PSMA-TAT is still necessary. Recently, de-escalated treatment protocols and application of actinium-225/lutetium-177-PSMA-617 "cocktail"-regimens improved the tolerability of [^{225}Ac]Ac-PSMA-617 TAT, reducing the risk for development dry-mouth syndrome [12]. This opens new avenues for future application in earlier stage disease. Therefore, combining alpha (actinium-225) and beta (lutetium-177) radionuclides might minimize adverse effects, while preserving treatment efficacy.

In our study we conducted an *in vitro* analysis of the long-term effect of [^{225}Ac]Ac-PSMA-617 on the survival of prostate tumour cells of human origin, as well as the specificity of the radiopharmaceutical for PSMA-positive prostate cancer cells. Our *in vitro* characterization includes an assessment of antiproliferative effects, cell viability, binding and colony formation assay in PSMA+ and PSMA- cells.

On the other hand, we also studied the effect of the coadministration of PSMA-617 labelled with actinium-225 and lutetium-177 in a xenographic nude mice model bearing prostate cancer. The outcomes were mice survival and the quantification of the volumetric evolution and uptake of PSMA-positive human prostate tumour line (LNCaP) tumours. For this purpose four different groups were studied after treatment with [^{225}Ac]Ac-PSMA-617 and [^{177}Lu]Lu-PSMA-617 individually or in combination.

2. Material and methods

2.1. Reagents

All reagents were purchased from commercial sources, such as Sigma-Aldrich (St Louis, MO, USA) and Thermo Fisher Scientific (Pittsburgh, PA, USA), unless otherwise specified. Human prostate cancer cells, LNCaP (ATCC™ CRL-1740) and PC3 (ATCC™ CRL-1435), were originally purchased from ATCC and maintained in CUDIM. [^{177}Lu]$LuCl_3$ is acquired in both qualities, carried added and non-carried added, from Isotopia (Israel). PSMA-617 (L-Lysine, N2-[[[(1*S*)-1,3-dicarboxypropyl]amino]carbonyl]-N6-[3-(2-naphthalenyl)-N-[[trans-4-[[[2-[4,7,10-tris(carboxymethyl)-1,4,7,10-tetraazacyclododec-1-yl] acetyl]amino]methyl]cyclohexyl]carbonyl]-L-alanyl]-, N2-[[[(1*S*)-1,3-Dicarboxypropyl]amino]carbonyl) was acquired from CMR (Russia) and JPT (Germany). Actinium-225, nitrate in solid form, was received from the Isotope-Regional Alliance, Joint Stock Company, Isotope JSC (Russia).

2.2. Radiolabelling

[^{225}Ac]Ac-PSMA-617 was labelled in 0.1 mol.L^{-1} sodium ascorbate buffer with 10 nmol/MBq of PSMA-617 precursor, and then the reaction mixture was heated for 30 min at 95 °C. Radiochemical purity was performed by an instant thin-layer chromatography system (iTLC) in conjunction with high-pressure liquid chromatography (HPLC), collecting fractions each minute, and measuring after two hours the photopeak of Francium-218 in a solid scintillator detector (3″ × 3″ well-type NaI [Tl] solid scintillation detector coupled to a multichannel analyser, ORTEC). A EC250/4.6 NUCLEODUR 100–5 C18ec (M&N) column was used with a 1.0 mL/min flow and a gradient of 0 to 10 min from 5 to 95 % B and from 10 to 15 min 95%B. Mobile Phase A: sodium citrate buffer 100 mmol.L^{-1}, pH = 4.6; Mobile Phase B: acetonitrile.

[^{177}Lu]Lu-PSMA-617 labelling was performed in an Easyone synthesis module (Trasis) using the corresponding cassette. The precursor (PSMA-617) was added at a concentration of 15 nmol/GBq. Radiochemical purity control of the product was obtained by HPLC using a Mancherey-Nagel (EC250/4.6 Nucleodur 100–5 C18EC) column and solvents A- 0.1 % trifuoroacetic acid in water and B- 1 % trifluoroacetic in acetonitrile, using the following gradient: 0 to 15 min from 5 % to 70 % B and from 15 to 20 min at 70 % B. For colloid determination, an iTLC (Agilent) support was performed using ammonium acetate 1 mol.L^{-1}: methanol (1: 1) as mobile phase.

[^{18}F]F-AlF-PSMA-11 was produced and controlled according to our previously described method [13].

2.3. In vitro studies

2.3.1. Cell lines

The LNCaP cell line was maintained in RPMI 1640 media with stable glutamine (Capricorn Scientific) supplemented with 10 % FBS (Gibco) and 10 % of its own conditioned medium (complete media), along with 100 μg/mL streptomycin and 100 U/L penicillin G (Sigma, St Louis, MO). The PC3 cell line were maintained in high glucose (4.5 g/L) DMEM media (Capricorn Scientific) with stable glutamine along with 10 % FBS (Gibco), 100 μg/mL streptomycin and 100 U/L penicillin. The cells were passaged once per week, and the medium was changed at the same frequency. Approximately one week later, subculturing was carried out using 0.25 % trypsin plus 0.02 % EDTA solution (Gibco) in sterile phosphate-buffered saline (PBS). Both cell lines were maintained in a 37 °C incubator containing a water-saturated atmosphere with 5 % CO_2.

2.3.2. PSMA expression in cell lines

PSMA expression in the tested cell lines was verified by performing uptake assays with [^{18}F]F-AlF-PSMA-11, locally produced and controlled in our centre. LNCaP or PC3 cells were seeded in 24-well plates and used for experiments when confluence as monolayers was reached. On the day of the experiment, cells were exposed to 0.26 MBq of [^{18}F]F-AlF-PSMA-11 (triplicate wells per plate) and incubated for 40 or 60 min at 5 % CO_2 and 37 °C. To determine specific binding, 0.4 μg/well of unlabelled PSMA (1000× excess) was added to the corresponding wells. Non-specific binding was determined by immediately removing the media after 0.26 MBq of [^{18}F]F-AlF-PSMA-11 addition to some wells ($T = 0$ condition). After incubation, the media were collected and preserved in tubes combined with phosphate buffer from a posterior cell wash. Trypsin 0.25 %/ EDTA 0.02 % solution was added to each well and incubated for 10 min. After cell detachment, the cell solution was collected in different tubes combined with phosphate buffer from the posterior well wash. The activity of each fraction (containing the same volume) was measured in a gamma counter (a 3″ × 3″ well-type NaI [Tl] solid scintillation detector coupled to a multichannel analyser, ORTEC). The average cell density in both LNCaP and PC3 plates was determined in different wells using the sulforhodamine B (SRB) method, which is based on the measurement of cellular protein content [14]. Percentage cell uptake was determined using the sum of the activity measured in (media plus wash) and (cell solution plus wash) in each well, and normalized to the amount of protein content. Counts were corrected for decay; background and nonspecific binding ($T = 0$) activities were subtracted. A statistical analysis was carried out for each cell line using a one-way analysis of variance (ANOVA) with Tukey's multiple comparisons test from data obtained in two independent experiments.

2.3.3. Antiproliferative effects

The antiproliferative effect of [^{225}Ac]Ac-PSMA-617 was determined in LNCaP (PSMA +) and PC3 cells (PSMA -). Briefly, LNCaP or PC3 cells (30,000 cells/well) were seeded on 24-well plates in complete medium the day before the experiment and kept in a CO_2 incubator.

On the day of the experiment, cell medium was removed and different concentrations o f [^{225}Ac]Ac-PSMA-617 prepared in complete media (0–250 KBq in 1 mL/well) were added to each well. Blocking conditions were performed with 0.4 μg/well of PSMA-617 non-radiolabelled peptide (1000× excess). After 24 h incubation at 5 % CO_2 and 37 °C, radioactive medium was discarded, and fresh complete medium was added after one wash with sterile buffer phosphate. Plates were incubated for an additional seven days in the same conditions as before, and then cells were fixed with 10 % trichloroacetic acid (TCA) after one buffer phosphate wash. The antiproliferative activity of [^{225}Ac]Ac-PSMA-617 was assayed using the SRB assay. For this purpose, cells were treated with a solution of 0.4 % SRB in 1 % acetic acid for 30 min and then washed three times with 1 % acetic acid. Microscopy images (Nikon) were captured at this point to visualise the cell morphology under each condition (10×). The stained cells were dissolved in Tris base solution (10 mmol.L^{-1}) and manually shaken to solubilize the protein-bound dye. Absorbance at 570 nm was measured in a multiwell microplate reader (Thermo), including a blank control (Tris solution). The percentage of cell growth was calculated according to the following formula:

$$\frac{(\text{Mean abs.of sample–mean abs.blank}) \times 100}{\text{Mean abs.of control (0 KBq condition)–mean abs.blank}}$$

A statistical analysis was carried out using a two-way analysis of variance (ANOVA) with Sidak multiple comparisons test from data obtained in two independent experiments. IC_{50} values were calculated from the dose–response relationship between the radiopharmaceutical activity concentration and the percentage of cell growth using a non-lineal regression curve fit.

The antiproliferative effects of [^{177}Lu]Lu-PSMA-617 were also analyzed using this method. In this case, activity concentrations assayed were 1000× higher (0–100 MBq/mL) than for actinium-225, and it was assayed only in the LNCaP cell line in two independent experiments. Lutetium-177 activity concentrations were selected based on previous reports [15].

2.3.4. Binding assays

LNCaP or PC3 cells were seeded on 24-well plates in complete medium, as explained in Section 2.3.2, and the next steps were performed exactly as described there until the end of the experiment. After one wash with PBS, 0.25 % trypsin/0.02 % EDTA solution was added, and the cells were incubated for 10 min. After homogenization, 10 μL were seeded on Whatman paper N° 1/4 and left to completely dry until exposure overnight in a cassette to a phosphor screen BAS-MS (FUJIFILM) together with a standard [^{225}Ac]$AcCl_3$ curve. Scanning was performed using a Typhoon FLA 7000 (GE Healthcare) laser scanner. The gel analysis function was performed on dot blots from images obtained using Image software. Simple linear regression fit of dots areas of standard curve *vs.* activity concentration decay allowed us to interpolate remaining activity in cells and the bounded radioligand normalized to cell number.

2.3.5. Cell viability assay

LNCaP or PC3 cells were seeded on 24-well plates in complete media, as explained in 2.3.2, and the next steps were performed exactly as described there until seven days of incubation were over. Then, MTT salt (3-(4,5-Dimethylthiazol-2-yl)-2,5-Diphenyltetrazolium Bromide) was added to each well at 0.5 mg/mL concentration, and plates were incubated at 5 % CO2 and 37 °C for approximately 30 min for LNCaP cells and 60 min for PC3 cells. Media was discarded, and MTT crystals were dissolved in dimethyl sulfoxide (DMSO) for reading at 570 nm in a multiwell microplate reader (Thermo). Cell viability was calculated according to the following formula:

$$\frac{(\text{Mean abs.of sample}) \times 100}{\text{Mean control (0 KBq condition)}}$$

A statistical analysis was carried out using a two-way analysis of variance (ANOVA) with Sidak multiple comparisons test from data obtained in two independent experiments. LD_{50} values were calculated from the dose–response relationship between the radiopharmaceutical concentration and the percentage of cells killed using a non-lineal regression curve fit.

2.3.6. Colony formation assay

LNCaP or PC3 cells were harvested and counted to incubate 100,000 cells in 1 mL 20 mmol.L^{-1} HEPES buffered culture media with different concentrations of [^{225}Ac]Ac-PSMA-617 or [^{225}Ac]Ac^{3+} in tubes. The tubes were incubated for 3 h at 5 % CO2 and 37 °C with manual rotation every 15 min. After incubation and homogenization, 1000 cells in 2 mL of complete media were seeded in 6-well plates and set to grow colonies for seven days in a humidified 5 % CO2 incubator. Next, plates were washed with phosphate buffer, fixed with 10 % TCA and stained with 0.4 % SRB/1 % acetic acid solution for 30 min. Colonies were manually counted using a stereomicroscope (Nikon), and the percentage of survival was calculated using the negative control (untreated cells) as 100 %. The area under the curve (AUC) was calculated using GraphPad 9.5.1 software. A statistical analysis was carried out using a two-way analysis of variance (ANOVA) with Sidak's multiple comparisons test from data obtained in two independent experiments.

2.3.7. Statistical analysis

All statistical analysis was performed using GraphPad 9.5.1 software. Values were considered significant at a *P* value of 0.05 or less.

2.4. Animal study protocols

All protocols for animal experimentation were performed in accordance with institutional, national and international guidelines for the use of animals, with the approval of the CUDIM Bioethics Committee's requirements (protocol number: 23071301) and under the current ethical regulations of the national law on animal experimentation No. 18.611 (Commission of ethics for animal studies (CEUA); National commission of experimentation with animals (CNEA) which is based on the principles and standards of the European Union Directive 2010/63/EU on the protection of animals used for scientific purposes.

2.5. Cell transplantation

Ten- to twelve-week-old male athymic nude mice (J:Nu-Foxn1nu, homozygous) were subcutaneously implanted in the left flank with 5 × 10^6 LNCaP cells (150 μL, 1:1, v:v, Cells in RPMI 1640:GeltrexTM). A small portion of testosterone gel (Androgel 50 mg /5 g) was applied daily to the skin of the mice until the appearance of tumours as a small dark-blue dot. Tumour growth was monitored by external caliper measurements [(short axis)2 x (long axis) x π]/6] and by PET-CT imaging with [^{18}F]F-AlF-PSMA-11 over two months. Animals were housed in racks with filtered air under controlled conditions temperature (24 ± 1) °C and relative humidity (40–60 %). They were maintained on a 14:10 h light/dark cycles at CUDIM's~~udim~~ animal facility with food and water *ad libitum*.

2.6. Protocol design

Treatment with radiopharmaceuticals [^{225}Ac]Ac-PSMA-617 and [^{177}Lu]Lu-PSMA-617 were carried out intravenously. Four groups were studied: one for each individual treatment of each radiopharmaceutical (groups 1 and 2), one based on a combination of both

radiopharmaceutical (group 3) and a control one (group 4). Average activity was 98 ± 5 KBq for [^{225}Ac]Ac-PSMA-617; 102 ± 18 MBq for [^{177}Lu]Lu-PSMA-617; 36 ± 9 KBq and 37.0 ± 8.7 MBq respectively when both radiopharmaceuticals [^{225}Ac]Ac-PSMA-617 + [^{177}Lu]Lu-PSMA-617 were co-administered. In all cases maximum volume to be injected was 0.2 mL.

The number of mice per group was 9 for control and lutetium-177 groups and 10 for actinium-225 and actinium-225 + lutetium-177 groups. Radiopharmaceuticals were administered intravenously *via* main tail vein once tumours reached a volume of 25–300 mm^3, approximately 3–8 weeks post inoculation.

The acceptance criteria for treatment application were the existence of a palpable tumour and a tumour volume <2 mm^3.

Availability for both radioisotopes (actinium-225 and lutetium-177) established rigid times for the application of the treatment, which prevented the adjustment of these times to the standardization of the observed individual tumour evolution. Also, the optimization of the number of mice exposed to inoculation and treatments prevented the application of a more limited criterion for tumour volume. However, adjusting the inoculation times in relation to the time of treatment application allowed for a similar initial tumour volume across groups (mean Vol, Table 1). The baseline prior to treatment administration was measured by [^{18}F]F-AlF-PSMA-11 PET for tumour characterization as described later.

2.7. Monitoring of therapeutic response

Therapeutic response was followed by *in vivo* imaging studies with a reference radiotracer for prostate cancer ([^{18}F]F-AlF-PSMA-11),which was administered both prior to radiotherapeutic treatment to assess baseline tumour uptake, and during follow-up to monitor therapeutic response. Tumour growth was also measured externally by caliber and recorded after the acquisition of each PET/CT study. Characterization was performed weekly, evaluating the different tumour stages; pre-treatment week (all groups), and post-treatment weeks 1, 2, 4, and 8 ([^{225}Ac]Ac-PSMA-617 and/or [^{177}Lu]Lu-PSMA-617). The control group was followed weekly (weeks 0, 1, 2 and 3) until its sacrifice was necessary due to tumour growth. Mouse sacrifice was determined individually based on the evaluation of the appearance of the tumour. The criterion used was caliber measured tumour size >3000 mm^3 and/or ulcerations in the tumour skin. In these cases, the animal was classified as non-survivor. Besides, if mice reached the 8th week with a non-palpable tumour it was sacrificed and classified as a survivor. For PET imaging, administration of the radiopharmaceutical was intravenous [maximum volume injected 0.2 mL, activity (45.4 ± 9.5) MBq, through the caudal tail vein] all animals of the 4 groups detailed above were used.

Small animal PET-CT imaging was performed in a nanoScan ® PET/CT Mediso Preclinical Imaging, based on LYSO scintillator. The spatial resolution of the scanner is 0.9 mm and the transaxial field of view (FOV) is 10.0 cm. The data were acquired in list mode in a 212 × 212 × 235 matrix with a pixel size of 0.4 × 0.4 × 0.4 mm and a coincidence window width of 1.0 nsec.

PET images (static studies) acquisition started 30 min after the bolus injection of [^{18}F]F-AlF-PSMA-11 for each mouse, the acquisition time was 40 min, followed by the CT scan of each animal (time approximately 2 min). During the whole period under study the animals remained sedated by inhalation with 2.5 % Isoflurane at an O_2 flow of (1.5–2.0) L/min. Sinograms were reconstructed using 3D maximum likelihood expectation maximization (3D-MLEM) with 4 iterations and 6 subsets.

2.8. Quantification

Tumour segmentation was performed on PET images by applying a semi-automatic algorithm (Region Growing, PMOD 3.8 Technologies, Ltd., Zurich, Switzerland) to define the volumes of interest (VOIs). The

Table 1
Summary of the average data and standard deviation calculated from the tumour quantifications for each treatment group, at each acquisition time. It contains the average TNr (target-no target relation), Volume and Sum values and standard deviation for each treatment and time, as well as the values normalized to the acquisition prior to treatment. In addition, the data on % survival in each group and % tumour detectability in the PET image were incorporated. This last data provides an idea of the success performance of the treatment.

Group	Acquisition week	N	Tumour detected [%]	Survival rate [%]	Mean TNr	SD TNr	Mean TNr norm (t0)	SD TNr norm (t0)	Mean Vol (cm3)	SD Vol (cm3)	Mean Vol norm (t0)	SD Vol norm (t0)	Mean SUM TNr	SD SUM TNr	Mean SUM TNr norm	SD SUM TNr norm
Control	0	9	100	100	4.62	1.36	1.00	0.00	0.13	0.06	1.00	0.00	0.59	0.31	1.00	0.00
	1	9	100	100	7.28	1.79	1.71	0.63	0.24	0.10	2.43	1.73	1.75	0.75	3.70	1.99
	2	9	100	100	7.64	3.24	1.83	1.01	0.38	0.22	3.91	3.43	3.32	3.28	6.76	4.72
	3	5	100	56	4.62	1.26	0.91	0.23	0.53	0.27	7.34	6.54	2.33	1.16	6.26	5.61
	4	0	–	0	–	–	–	–	–	–	–	–	–	–	–	–
[^{177}Lu]Lu-PSMA-617	0	9	100	100	5.38	1.02	1.00	0.00	0.12	0.07	1.00	0.00	0.61	0.36	1.00	0.00
	1	9	100	100	4.08	0.80	0.79	0.24	0.09	0.06	0.93	0.51	0.39	0.33	0.77	0.51
	2	9	100	100	4.78	3.09	0.95	0.73	0.07	0.05	0.78	0.55	0.41	0.44	0.86	0.76
	4	9	89	100	3.52	2.42	0.72	0.57	0.13	0.16	1.77	2.56	0.55	0.63	1.39	1.58
	8	9	78	33	2.85	2.14	0.58	0.46	0.66	0.85	7.47	9.54	2.70	3.66	6.10	6.97
[^{225}Ac]Ac-PSMA-617	0	10	100	100	4.62	1.61	1.00	0.00	0.13	0.08	1.00	0.00	0.65	0.47	1.00	0.00
	1	10	100	100	4.22	1.64	0.89	0.12	0.10	0.07	0.71	0.20	0.43	0.35	0.65	0.21
	2	10	100	100	3.87	1.55	0.96	0.43	0.08	0.05	0.69	0.41	0.39	0.42	0.66	0.56
	4	10	100	90	2.56	0.97	0.64	0.27	0.07	0.07	0.50	0.36	0.22	0.34	0.34	0.34
	8	9	60	50	1.67	1.82	0.48	0.66	0.23	0.42	1.74	3.01	0.83	1.54	0.83	1.54
[^{177}Lu]Lu-PSMA-617 and [^{225}Ac]Ac-PSMA-617	0	10	100	100	4.30	1.76	1.00	0.00	0.08	0.04	1.00	0.00	0.37	0.32	1.00	0.00
	1	10	100	100	3.24	2.33	0.79	0.39	0.07	0.07	1.07	0.82	0.33	0.57	0.92	0.89
	2	10	100	100	2.51	2.18	0.61	0.39	0.04	0.06	0.57	0.61	0.22	0.49	0.51	0.70
	4	10	70	100	2.05	2.25	0.47	0.47	0.04	0.06	0.58	0.78	0.10	0.15	0.36	0.55
	8	10	60	90	1.20	1.26	0.28	0.27	0.02	0.04	0.25	0.29	0.06	0.15	0.12	0.16

implemented algorithm works through the region growth strategy, where a representative pixel of the region to be segmented is manually designated and by means of an acceptance or rejection criterion (intensity level within a threshold) the neighbors to said pixel are incorporated or discarded from the defined VOI. The algorithm performs this same evaluation iteratively, incorporating new pixels into the VOI in each cycle. This algorithm concludes with the growth of the VOI as long as no new pixels have been incorporated after the last iteration. From the VOIs defined in each mouse tumour and at each pre- and post-treatment acquisition time point, the tumour volume and the average and total radiopharmaceutical bind (sum) to tumour were calculated. Additionally, a contralateral spherical region of fixed size of 2 mm was manually defined to represent normal tissue nonspecific signal. The tumour/normal uptake ratio (TNr) was calculated from this data. The data were finally normalized to the initial volume and uptake of each tumour, prior to starting the treatment. Fig. 1 shows an example of determining VOIs by region growth.

3. Results

3.1. Radiolabelling

The radiochemical purity of [^{225}Ac]Ac-PSMA-617 was (97.7 ± 1.0)% ($n = 8$) 2 h after labelling (optimized time of quality control after the end of preparation) and (96.2 ± 1.1)% ($n = 4$) 24 h after labelling.

The radiochemical purity of [^{177}Lu]Lu-PSMA-617 was (99.3 ± 0.6)% ($n = 10$) 0.5 h after labelling (optimized time of quality control after the end of preparation) and (98.0 ± 0.5)% ($n = 5$) 48 h after labeling.

3.2. In vitro assays

3.2.1. PSMA expression in cell lines

To verify PSMA expression in our cell lines, uptake assays were performed using [^{18}F]F-AlF-PSMA-11. Incubation of [^{18}F]F-AlF-PSMA-11 in PC3 cells for 40 or 60 min showed negligible binding, while LNCaP cells exhibited high time-dependent uptake. Moreover, this binding was completely blocked with an excess of unlabelled PSMA-11 peptide (Fig. 2).

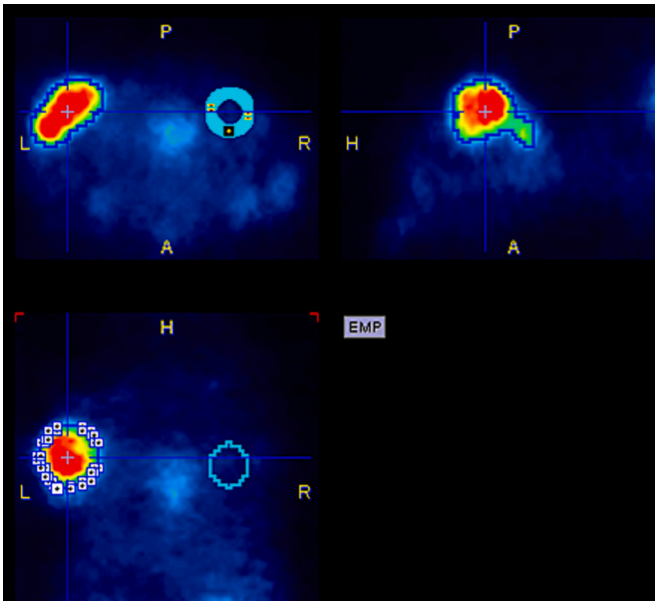

Fig. 1. Example of VOI determination by semi-automatic segmentation for tumour and manually for normal tissue in xenographic prostate mice tumour model by means of [^{18}F]-AlF-PSMA-11 PET image.

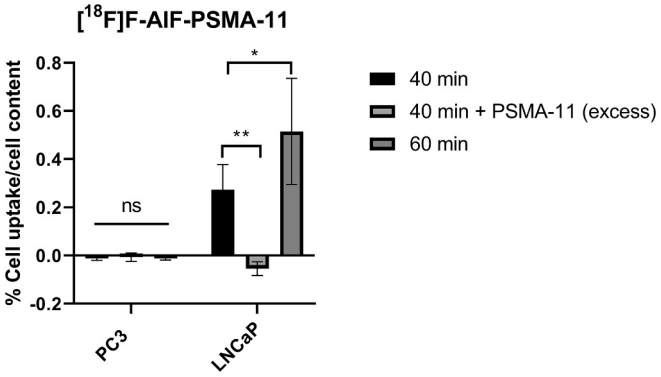

Fig. 2. Uptake of [^{18}F]F-AlF-PSMA-11 in PC3 and LNCaP cell lines after 40 min (with or without unlabelled PSMA-11 blocking) and 60 min of incubation. The counts were corrected for decay and normalized to the cellular protein content. The resulting values are expressed as the percentage of cell uptake normalized to cell content ± SD. *One-way ANOVA Tukey's multiple comparisons test: p** = 0,031; p* = 0.026; ns = non-significant.*

3.2.2. Antiproliferative effects

The long-term effect of [^{225}Ac]Ac-PSMA-617 over cell proliferation was studied *in vitro* using LNCaP (PSMA-positive) and PC3 (PSMA-negative) cell lines. Exposition of LNCaP cells to increasing concentrations of [^{225}Ac]Ac-PSMA-617 (0–250 KBq/mL) for 24 h and seven days in fresh media (without radiopharmaceutical) showed a dose-dependent inhibition in proliferation (Fig. 3A). Inhibition was evidenced from the lowest activity concentration tested and was significantly lower in LNCaP cells than in PC3 cells, until 5 KBq/mL. After 25 KBq/mL no differences in effect were observed between cell lines. The 50 % cell-growth inhibition (ID_{50}) calculated for PSMA+ cells (LNCaP) was 0.14 KBq/mL; instead, in cells where the antigen was not expressed (PC3), ID_{50} value was a two orders of magnitude higher (15.6 KBq/mL, Fig. 2B). Microscopic examination of the cells after each treatment revealed distinct differences in density and morphology in the LNCaP cells compared to the untreated control, even with the lowest activity tested. In contrast, reduced cell density and signs of cell death in PC3 cells were observed only at an activity concentration of 25 KBq/mL (Fig. 4). These results revealed that the expression of PSMA lead to a higher cell sensitivity to [^{225} Ac]Ac-PSMA-617 antiproliferative effects. Additionally, IC_{50} for [^{177}Lu]Lu-PSMA-617 in LNCaP was determined (Fig. 3C), yielding a value of 44 KBq/mL, >300 times higher than that achieved for Actinium-225-treated cells, which is consistent with previous reports [16].

3.2.3. Binding assays

Saturation binding studies in cells after 24 h incubation plus seven days in fresh media were analyzed by autoradiography assays. A dose-dependent binding to LNCaP cells was observed, while binding in PC3 was significantly lower at most activity concentrations (Fig. 5A and B). Unconjugated [^{225}Ac]Ac^{3+} at high activity concentration (35 KBq/mL) in both cell lines showed no differences in binding between them (Fig. 5B, Insert graph). In fact, when cells were also challenged with an excess of unlabelled PSMA-617 peptide, binding was reduced compared to the same condition without blocking (0.05 KBq/mL + B *vs.* 0.05 KBq/mL). However, binding was practically undetectable until 25 KBq/mL activity concentration in PC3 cells, and it was always one order of magnitude below LNCaP union. High affinity for LNCaP was one again observed for [^{225}Ac]Ac-PSMA-617 having a kd of 0.12 nmol, whereas kd in PC3 was 52 nmol (Fig. 5C).

3.2.4. Cytotoxic effect of [^{225}Ac]ac-PSMA-617

The cytotoxicity effect was determined through MTT assay in LNCaP or PC3 cells after 24 h of treatment with [^{225}Ac]Ac-PSMA-617 plus seven days in fresh media. A significantly higher cytotoxic and dose-dependent

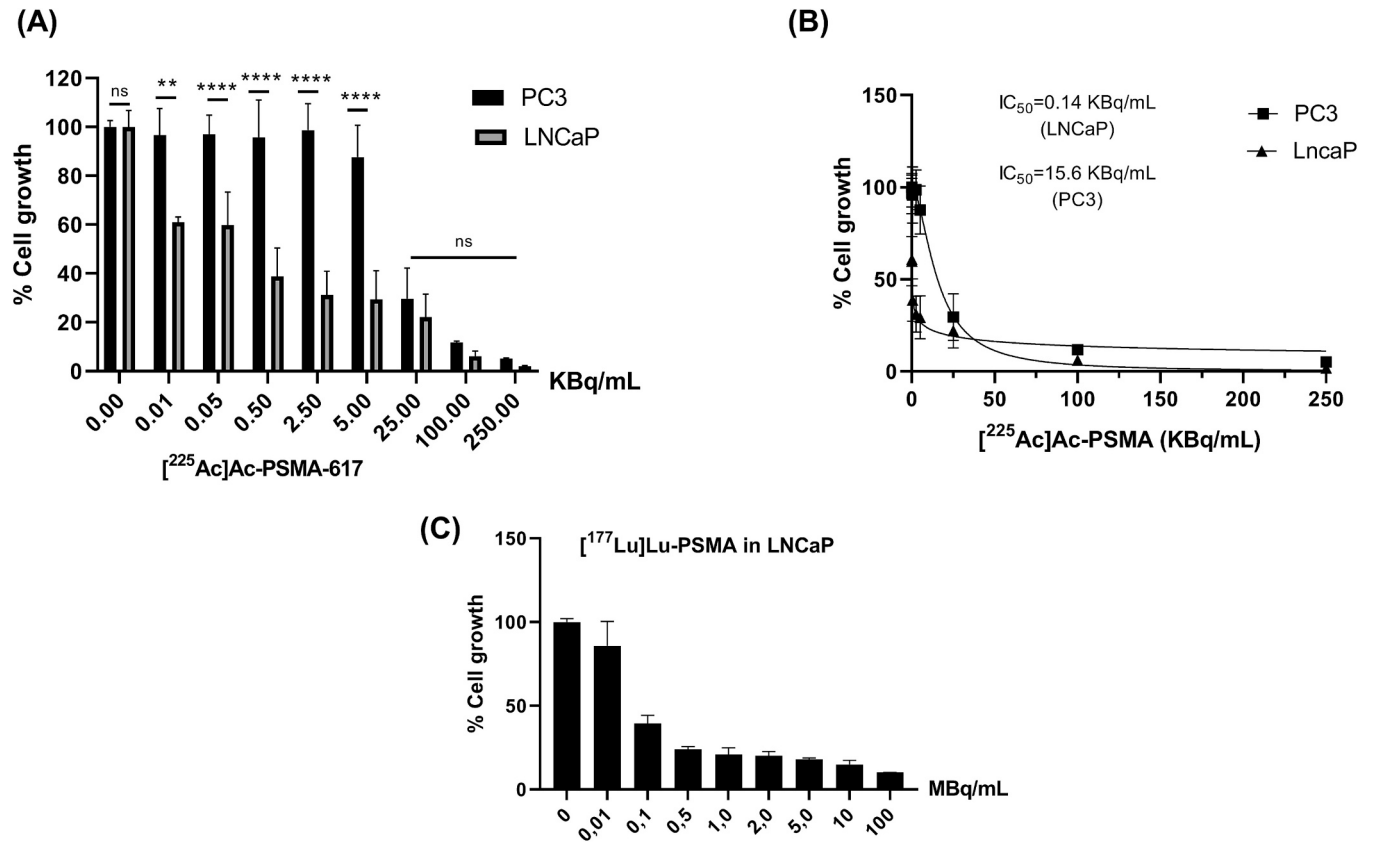

Fig. 3. A) Antiproliferative effect of increasing concentrations of [^{225}Ac]Ac-PSMA-617 (KBq/mL) over PC3 (PSMA -) or LNCaP (PSMA +) cell proliferation. *Two-way ANOVA Sidak multiple comparisons test: p** = 0,0098; p**** < 0.0001; ns = non-significate. Results obtained in two independent experiments.* **B)** Non-linear curve fit performed in GraphPad to calculate IC_{50} (50 % cell-growth inhibition) values for PC3 or LNCaP in response to [^{225}Ac]Ac-PSMA-617.
C) Antiproliferative effect of increasing concentrations of [^{177}Lu]Lu-PSMA-617 (KBq/mL) over LNCaP cell proliferation.

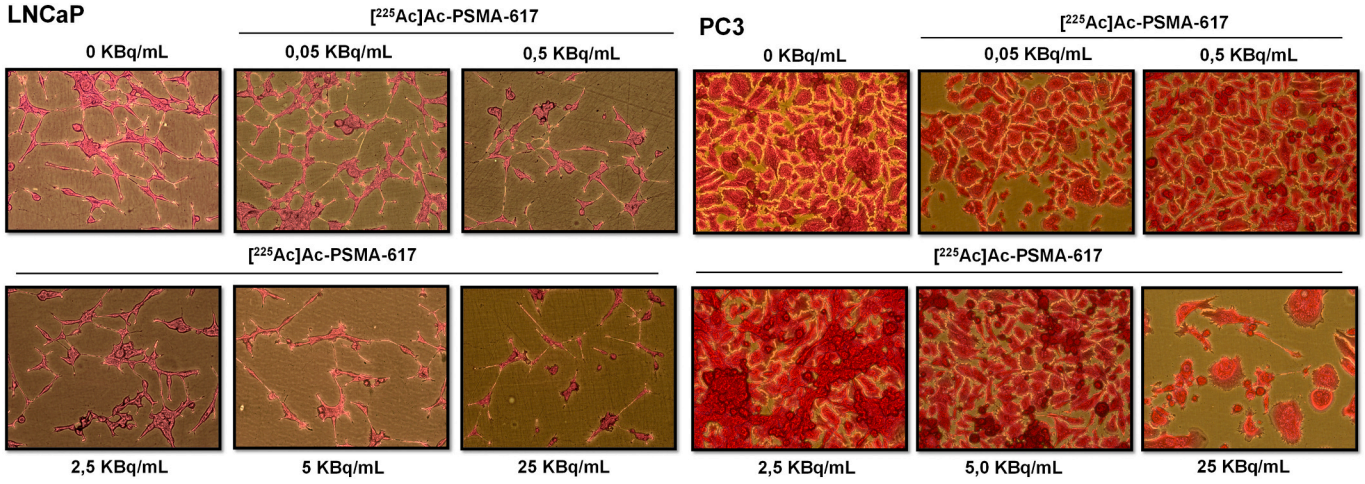

Fig. 4. Microscopy images captured after SRB staining in LNCaP or PC3 treated cells with [^{225}Ac]Ac-PSMA-617 to visualise cell morphology and density under each condition (10×).

effect of [^{225}Ac]Ac-PSMA-617 was observed from the lowest activity concentration tested in LNCaP (0.01 KBq/mL, $p = 0.022$) compared to PC3, in which a notorious cytotoxic effect was not found until the 25 KBq/mL treatment (Fig. 6A). Lethal doses calculated by this assay were LD50 = 0.045 KBq/mL for LNCaP and 9.08 KBq/mL for PC3. Furthermore, when we challenged LNCaP cells with 0.05 KBq/mL of [^{225}Ac]Ac-PSMA-617 in concomitant with unlabelled PSMA at molar excess, cell viability significantly increased (p = 0.022) (Fig. 6B). In fact, treatment with increasing concentrations of free [^{225}Ac]$AcCl_3$ had a similar cytotoxic effect between both cell lines, probing its unspecific effect (Fig. 6C).

3.2.5. *Clonogenic survival effect after treatment with [^{225}Ac]ac-PSMA-617*

Clonogenic survival after exposure with [^{225}Ac]Ac-PSMA-617 was analyzed. In Fig. 7A, representative photographs obtained from each condition at the end of the experiment are shown. The percentage of

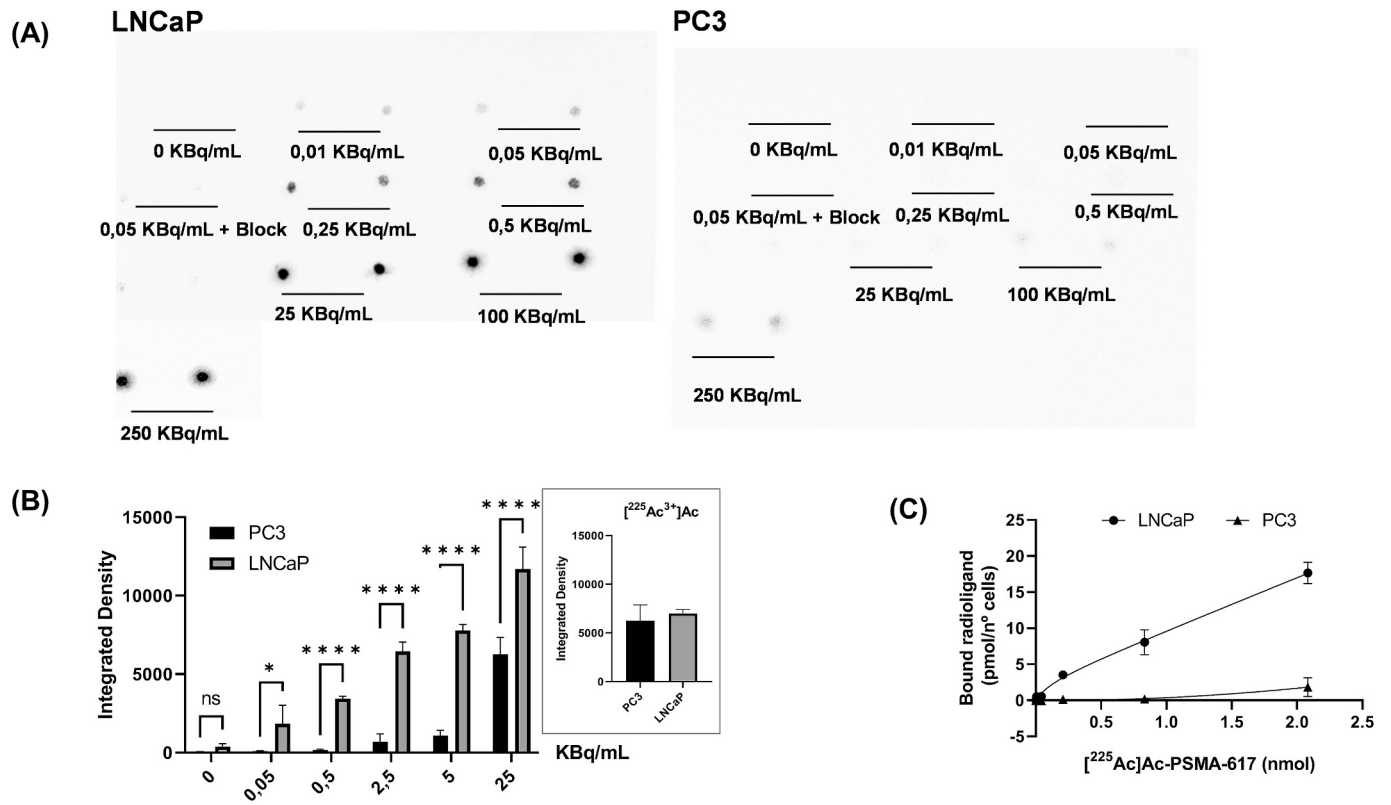

Fig. 5. A and B) Representative phosphorimager dot blots of PC3 or LNCaP cells that were incubated with increasing concentrations of [^{225}Ac]Ac-PSMA-617 (KBq/mL) are shown with their integrated density quantification using ImageJ (Graph). In insert, [$^{225}Ac^{3+}$]Ac binding (37 KBq/mL) was quantified in both cell lines. **C)** One-site saturation binding modelling in LNCaP and PC3 cells performed in GraphPad. *Two-way ANOVA Sidak multiple comparisons test; p**** < 0.0001; ns = not significant.*

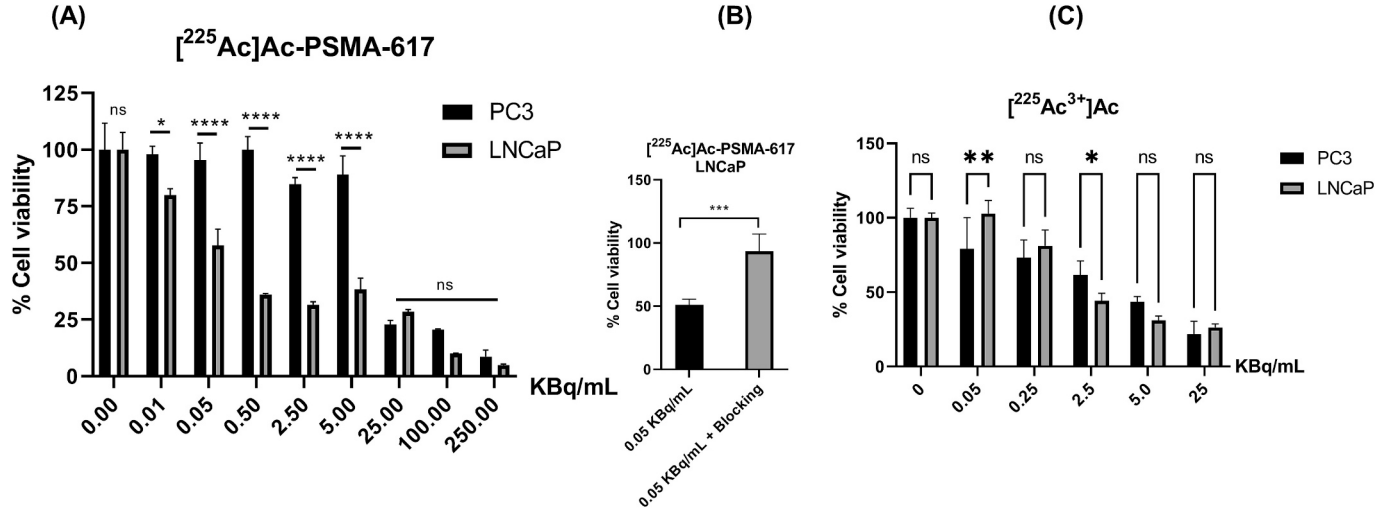

Fig. 6. A) Cytotoxic effect of increasing activity concentrations of [^{225}Ac]Ac-PSMA-617 in LNCaP or PC3 measured by MTT assay. *Two-way ANOVA Sidak multiple comparisons test *p = 0,022; p**** < 0,0001; ns = not significant.* **B)** LNCaP cell viability in the presence of a molar excess of unlabelled PSMA-617 and 0.05 KBq/mL [^{225}Ac]Ac-PSMA-617. *One-way ANOVA Tukey test; ***p = 0.004.*
C) Cytotoxic effect of increasing the activity concentrations of free [$^{225}Ac^{3+}$]Ac in LNCaP or PC3 cell lines. *Two-way ANOVA Sidak multiple comparisons test: **p = 0.027; *p = 0.049; ns = not significant.*

colony survival decreased significantly ($p < 0.0001$) in LNCaP cells treated with 1 KBq/mL and 10 KBq/mL, as compared to PC3 cells treated with the same activity concentrations (AUC for LNCaP curve: 1151 ± 142 *vs.* PC3: 2906 ± 302) (Figs. 7A and B). At a high dose, no colony survival was observed in either cell line (Fig. 5B). Colony formation was also assessed with non-conjugated [^{225}Ac]$AcCl_3$Ac in LNCaP cells evidencing significantly higher colony survival compared to the radiopharmaceutical at the same activity concentration ($p < 0.0001$) (Fig. 7C).

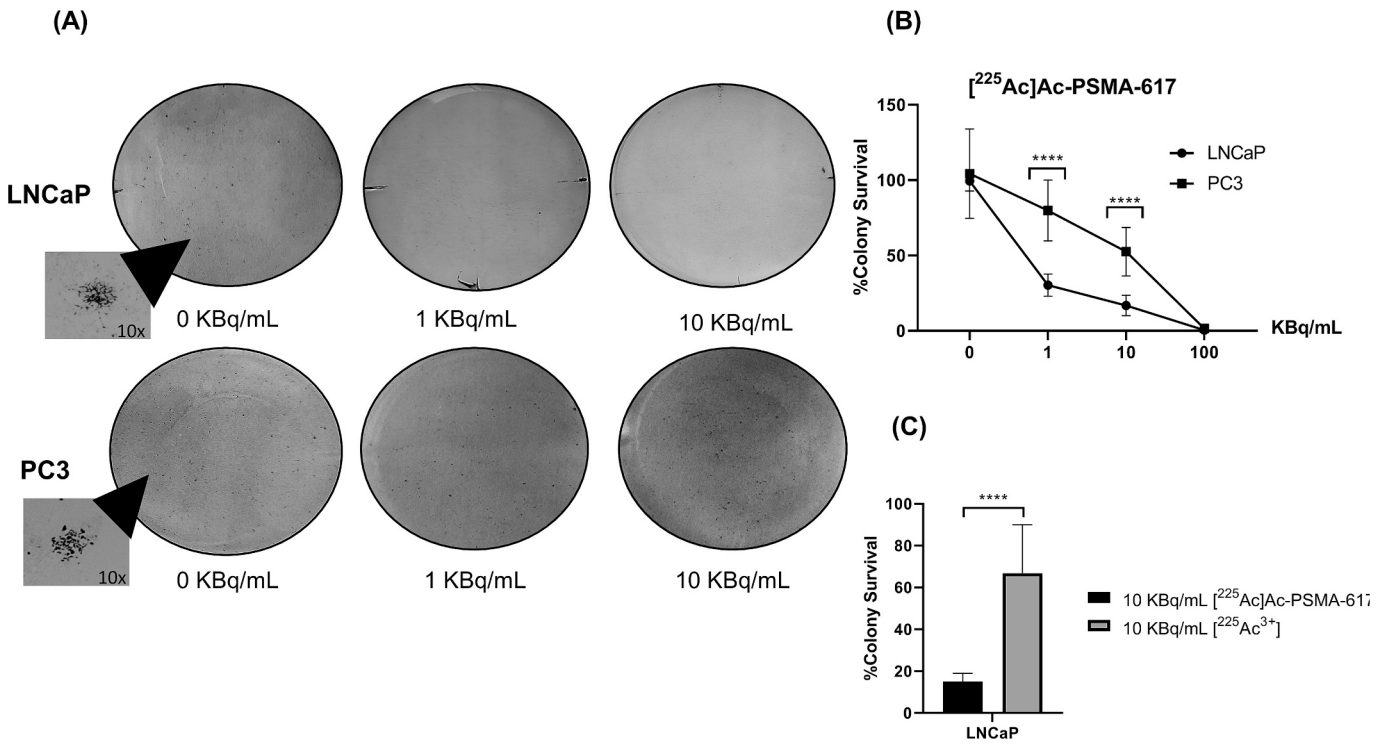

Fig. 7. Clonogenic survival effect after 3 h of treatment with [225Ac]Ac-PSMA-617 in LNCaP or PC3. A) After seven days, colonies were captured and visualized in photographs as black dots. Stereomicroscope images (10×) of a representative colony are shown for LNCaP and PC3. B) Calculated percentage of colony survival in each condition for each cell line. The 0 KBq/mL condition corresponds to 100 % survival for each cell line. Two-way ANOVA Sidak multiple comparisons test; **** < 0.0001. C) Calculated percentage of colony survival in LNCaP after 10 KBq/mL treatment with [225Ac]Ac-PSMA-617 *vs.* [225Ac3+]Ac. Unpaired *t*-test; **** < 0,0001.

3.3. *In vivo assays*

Treatments with the radiopharmaceuticals [^{225}Ac]Ac-PSMA-617 and [^{177}Lu]Lu-PSMA-617 individually, or a combination of both, were successfully carried out in a xenographic mice model. Figs. 8 and 9 show the tumour growth at 7 and 30 days, respectively, after treatment was performed, monitored by [^{18}F]F-AlF-PSMA-11 PET image. The weekly evolution of normalized tumour volume was evaluated for each treatment (Fig. 10).

The summary of the average data and standard deviation calculated from the tumour quantifications for each treatment group, at each acquisition time is shown in Table 1. It contains the average TNr (target-no target relation), Volume and Sum values and standard deviation for each treatment and time, as well as the values normalized to the acquisition prior to treatment. In addition, the data on % survival in each group and % tumour detectability in the PET image were incorporated. This last data provides an idea of the success performance of the treatment.

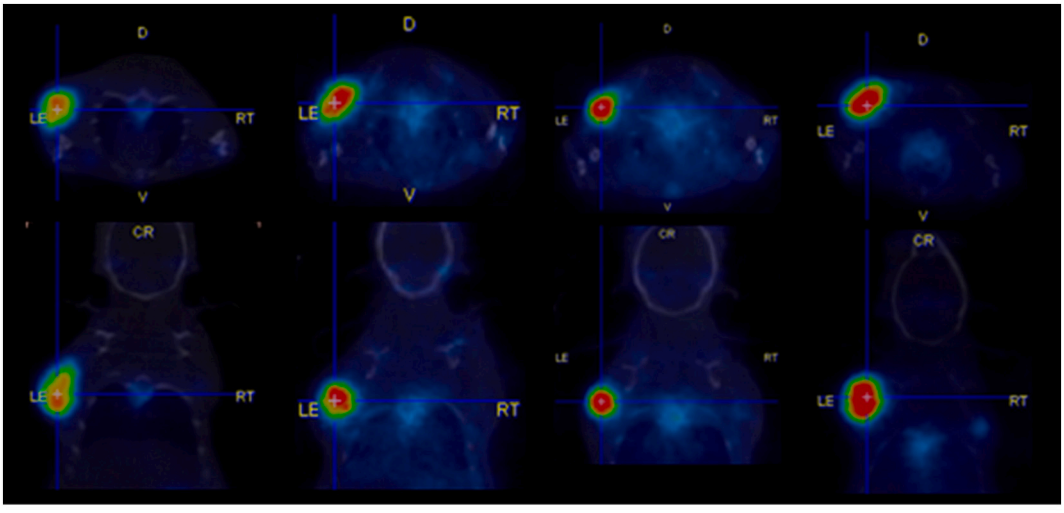

Fig. 8. Representative [^{18}F]AlF-PSMA-11 PET image of each treatment group 7 days after treatment.

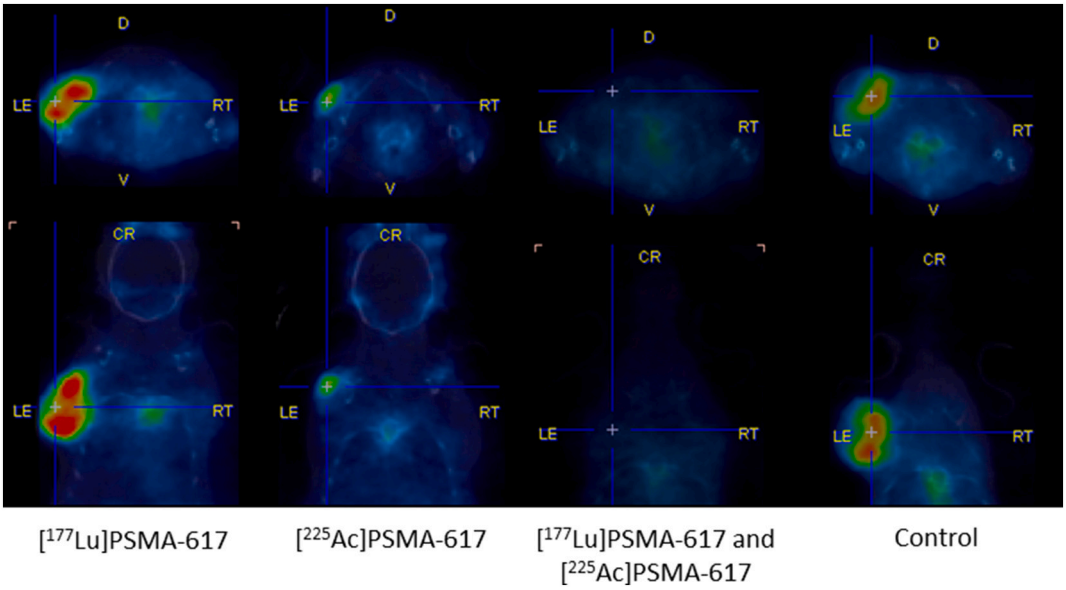

Fig. 9. Representative [^{18}F]AlF-PSMA-11 PET image of each treatment group 30 days after treatment.

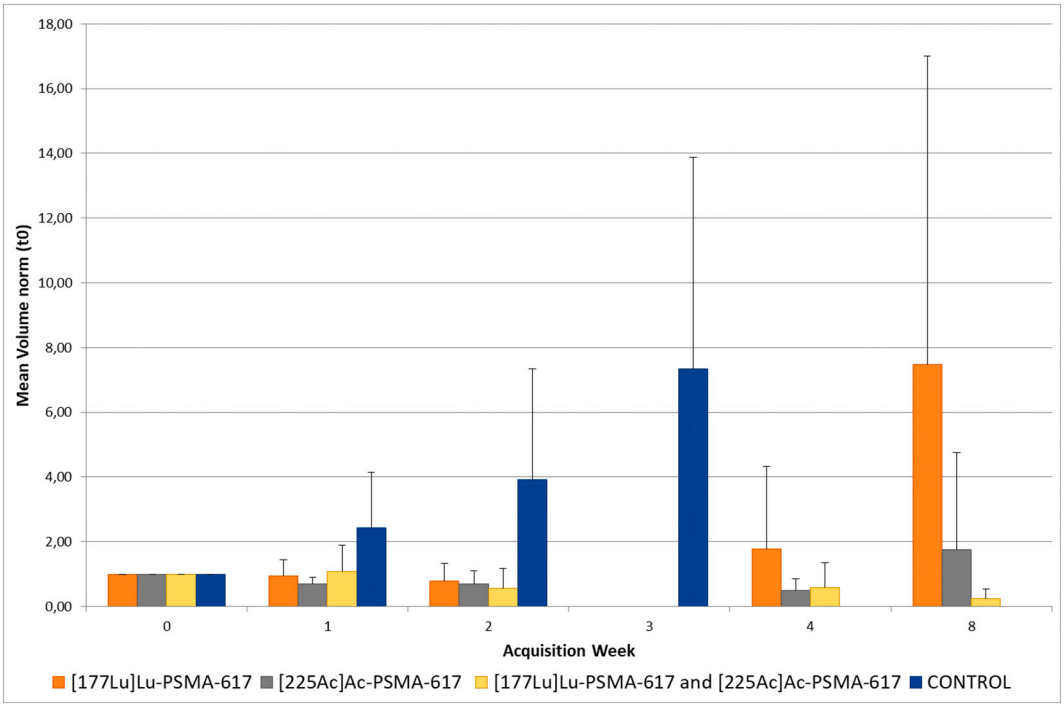

Fig. 10. It is shown the evolution of normalized tumour volume in 0–8 week after each treatment. Continuous tumour expansion was observed in all mice in the control group. The maximum volume was observed in week 3, when the mice were sacrificed, as established in the protocol. Error bar corresponds to 1sd. $N = 9$ for control and lutetium-177 groups; $N = 10$ for actinium-225 and (actinium-225 + lutetium-177) groups.

In the control group, all mice showed a continuous expansion of the tumour. Maximum volume was observed at week 3, when they were sacrificed as established in the protocol. In groups that received a single dose of [^{177}Lu]Lu-PSMA-617 or [^{225}Ac]Ac-PSMA-617, an initial reduction of tumour volume was verified, followed by a rapid tumour development between weeks 4 to 8. This effect was more notorious with [177Lu]Lu-PSMA-617 treatment. As verified in the standard deviation values associated with the graph, it is important to highlight that this evolution is notoriously uneven between the subjects of the same treatment, which includes mice with total tumour reduction or remission, where the tumour is no longer detectable by the imaging method, as well as absence of palpable tumour by week 8. In the combined treatment with both radiopharmaceuticals, tumour volume decreased over weeks, being undetectable in 40 % of subjects at week 8.

Weekly evolution of the average binding of the radiopharmaceutical to the tumour volume was evaluated as total sum uptake and TNr, for each treatment, both measurements normalized to the prior treatment quantity (Fig. 11A and B).

The overall efficiency of the treatments is shown in Fig. 12 representing survival and tumour detectability rates. In the control group, tumour detectability was 100 % in all acquisitions and the survival rate was 60 % in week 3 and 0 % in week 4.

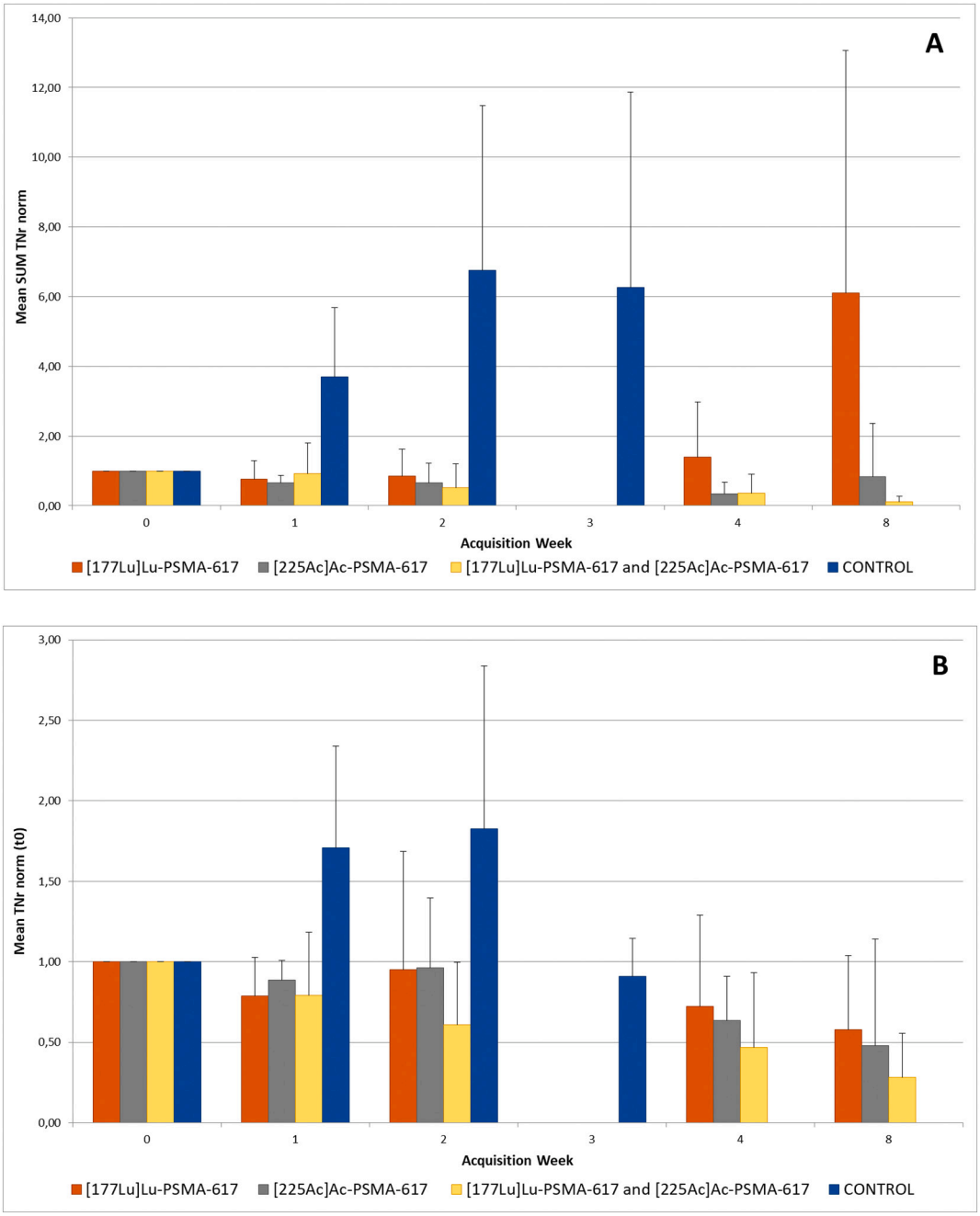

Fig. 11. Weekly evolution of the average binding of the radiopharmaceutical to the tumour volume, which was evaluated as total sum uptake (A) and TNr (B). For each treatment, both measurements were normalized to the pre-treatment quantity. Error bar corresponds to 1sd. N = 9 for control and lutetium-177 groups; N = 10 for actinium-225 and (actinium-225 + lutetium-177) groups.

4. Discussion

Since prostate-specific membrane antigen tracer [^{68}Ga]Ga-labelled PSMA-11 emerged as a new positron emission tomography (PET) tracer for prostate cancer [17], a new PSMA-617 ligand was developed and optimized for PSMA-targeted radioligand therapy [18]. [^{177}Lu]Lu-PSMA-617 is a radioligand therapy that delivers β-particle radiation to PSMA-expressing cells and the surrounding microenvironment, increasing overall survival in patients with advanced PSMA-positive metastatic CRPC [19]. Unfortunately, about 30 % of patients do not respond to [^{177}Lu]Lu-labelled PSMA ligands [20]. Even more, β-particles low LET and a large range in tissues are considered disadvantages in terms of effectiveness against metastatic cancers. Targeted alpha therapy using actinium-225 is emerging as a novel therapy for patients with metastatic CRPC and could provide a more effective therapy strategy compared to [^{177}Lu]Lu–PSMA-617. High LET and short tissue penetration of actinium-225 provide localized dose effects and high local toxicity, making it desirable for treatment of metastatic cancers [21]. However, preclinical assessments of newly developing Actinium-225 radiopharmaceuticals, such as [^{225}Ac]Ac-PSMA-617, including different *in vitro* characteristics, are still lacking.

Our work demonstrates the usefulness of an *in vitro* characterization analysis that provides relevant information for exploring and comparing the *in vitro* efficacy of current and future [^{225}Ac]Ac-PSMA-targeting tracers. The objective of this work was to evaluate the *in vitro* biological long-term effect of [^{225}Ac]Ac-PSMA-617 on the proliferation and

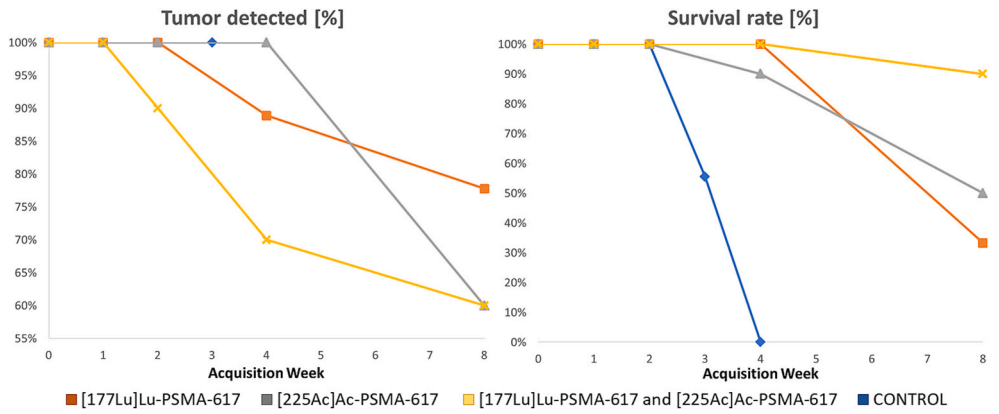

Fig. 12. Overall efficiency of the treatments by plotting survival and tumour detectability rates. In the control group, tumour detectability was 100 % in all acquisitions, and the survival rate was 60 % in week 3 and 0 % in week 4. N = 9 for control and lutetium-177 groups; N = 10 for actinium-225 and (actinium-225 + lutetium-177) groups.

survival of prostate tumour cells of human origin, as well as to evaluate the specificity of the radiopharmaceutical for PSMA-positive prostate cancer cells.

To this end, we performed an *in vitro* analysis of [^{225}Ac]Ac-PSMA-617 to report *in vitro* characteristics, such as cell binding and biological long-term effects. Using sulforhodamine B staining as a viable, fast and easy technique to assess cell proliferation, we showed a significantly higher antiproliferative effect of [^{225}Ac]Ac-PSMA-617 in LNCaP cells (PSMA +) over PC3 cells (PSMA -) from the lowest concentration tested (0.01 KBq/mL), until 5 KBq/mL condition after one week of radiopharmaceutical exposure. After 25 KBq/mL, no differences in effect were observed between cell lines, which is probably related to the high exposition of cells to radiation, independently of antigen expression. The activity concentration that results in cell growth inhibition of half of the cells (IC_{50}) evidenced that lower activity concentrations of [^{225}Ac]Ac-PSMA-617 are sufficient for inducing cell growth inhibition effects in LNCaP cells compared to PC3 cells (LD_{50} for LNCaP = 0.14 KBq/mL *vs* PC3 = 15.6 KBq/mL). Moreover, when we visualized LNCaP-stained cells in microscopy after each treatment, clear differences in density were evidenced from the lowest activity tested in comparison with the un-treated condition, as expected. Furthermore, the morphology of the cells was altered, showing changes from fusiform and polygonal to rounded or shapeless cells. Instead, PC3 reduced density, and formless cells were only monitored from 25 KBq/mL. Additionally, IC_{50} for [^{177}Lu]Lu-PSMA-617 in LNCaP was >300 times higher than that achieved for actinium-225-treated cells, which is consistent with previous reports [16]. Our results imply that [^{225}Ac]Ac-PSMA-617 presents a specific *in vitro* antiproliferative effect on prostate cancer cells that express the PSMA antigen, which confirms that the actinium-225 radionuclide does not interfere with the binding or uptake of PSMA-617 peptide. We also showed dose-dependent binding of [^{225}Ac]Ac-PSMA-617 to LNCaP cells using novel dot blot autoradiography assays, while binding in PC3 cells was insignificant at the same activity concentrations. These results corroborate that antiproliferative effects are mediated by [^{225}Ac]Ac-PSMA-617 binding/internalization to cells and are specific to PSMA expression. In fact, when LNCaP cells were challenged with an excess of unlabeled PSMA, binding was significantly reduced compared to the same condition without blocking. Furthermore, when cells were exposed to unconjugated actinium-225, there were no significant differences in uptake between cell lines. Metabolically active cells remaining after exposure with [^{225}Ac]Ac-PSMA-617 were analyzed using the MTT method. Briefly, MTT is a colorimetric assay based on the quantification of purple formazan produced in living cells as a result of the yellow tetrazolium salt by NAD(*P*)H-dependent oxidoreductase enzymes. The lethal dose calculated by this assay for [^{225}Ac]Ac-PSMA-617 in LNCaP was even smaller than that calculated with the SRB method (LD_{50} = 0.045 KBq/mL with MTT *vs.* 0.14 KBq/mL with SRB), indicating that some percentage of stained cells that remained attached to the well were not viable. These results empower the use of both techniques when analysing the radiopharmaceutical effect on cell proliferative capacity and viability. In this sense, significant differences in cell viability were found between LNCaP and PC3 cells at every concentration in the range of 0.01 and 5.0 KBq/mL, corroborating that [^{225}Ac]Ac-PSMA-617 is significantly more cytotoxic when the antigen is present. Beyond 25 KBq/mL treatment, the cell-specific effect was lost, as was also observed in the antiproliferative assays. Furthermore, the viability of the cells was augmented significantly when unlabelled PSMA excess was added together with 0.5 KBq/mL [^{225}Ac]Ac-PSMA-617 in LNCaP cells (approx. 90 % viability with blocking *vs.* 50 % viability without blocking). Unconjugated [^{225}Ac]Ac^{3+} effect was not shown to be dependent on the cell line.

It is expected that the Actinium radiopharmaceutical affects the capacity of a cell to produce a colony as a result of damage to chromosomes and apoptosis pathways. When we tested the clonogenic survival of LNCaP or PC3 cells after exposure to 1 KBq/mL or 10 KBq/mL of [^{225}Ac]Ac-PSMA-617, LNCaP colonies were dose-dependently reduced; in contrast, the PC3 colonies were reduced significantly less. With 100 KBq/mL treatment, 0 % survival was observed for both LNCaP and PC3, again indicating that the cell-specific effect was lost at high activity concentrations. Even more, when LNCaP cells were challenged with 10 KBq/mL of free [^{225}Ac]$AcCl_3$, percentage of survival was significantly higher compared to 10 KBq/mL of [^{225}Ac]Ac-PSMA-617, proving again that the effect of [^{225}Ac]Ac-PSMA-617 is PSMA-ligand dependent.

The other objective of this work was to study the effect of the coadministration of PSMA-617 labelled with actinium-225 and lutetium-177 *in vivo* in a xenographic nude mice model bearing prostate cancer, since 177-Lutetium-PSMA therapy combined with low-activity 225-actinium-PSMA is emerging as a promising treatment option. In this sense, our *in vivo* studies are in agreement with this positive effect of combined therapies with Lutetium-177 and Actinium-225 radiopharmaceuticals.

In the control group, consistent with the volume behavior, an increase in the average binding of the radiopharmaceutical is observed. In the final week, this value was reduced, which could be due to presence of necrotic regions in the tumour. These regions are characteristic of rapidly growing tumour processes and do not present radiopharmaceutical affinity receptors.

For the three proposed treatments, average binding decreases along weeks. The volume increase observed in the final weeks for individual treatments, does not correspond to an increase in the average binding, as in the case of the control group due to presence of necrotic regions. Despite these regions, total binding varies with strong correlation to

volume, as can be verified on Fig. 9 and Fig. 10.

In order to characterize global efficiency of the treatments analyzed, plots of survival and detectability % were made (Fig. 12). In the control group, tumour detectability was 100 % in all acquisitions and the survival rate was 60 % at week 3 and 0 % at week 4.

In individual treatments of lutetium-177 and actinium-225 up to week 4 the survival rate is 100 % and then drops to 40 and 50 % respectively in week 8. Tumour detectability in these individual treatment groups initially decreases to 90 % for lutetium-177 at week 4, remaining at 100 % for actinium-225. By week 8, a decrease in detectability was observed in both groups, being 80 % for lutetium-177 and dropping abruptly to 60 in the case of actinium-225.

In relation to the combined treatment of actinium-225 and lutetium-177, the best performances are observed in relation to tumour detectability, showing a high remission rate and the best survival percentage in the evaluated periods.

5. Conclusions

Long-term effects of [^{225}Ac]Ac-PSMA-617 in human prostate cancer cells *in vitro* proved to be specific for PSMA positive cells in terms of their antiproliferative effects, binding characteristics, cytotoxicity and clonogenic survival.

A four branch preclinical study with ([^{177}Lu]Lu-PSMA-617 and [^{225}Ac]Ac-PSMA-617) or its combination was successfully performed. This preclinical protocol represented a very important challenge to coordinate deliveries of actinium-225 and lutetium-177 and the xenographic prostate cancer evolution. [^{18}F]F-AlF-PSMA-11 was a suitable PET probe to monitor tumour growth along 30 days after tumour was palpable. The co-administration of both beta and alpha therapeutical radiopharmaceuticals showed the best results in terms of survival, growth rates and absence of tumour at the endpoint of the study. PSMA RIT and TAT combined therapy opens doors to a better future for patients, in case the disease progression could be delayed as shown in this preclinical study. Our results could contribute to broadening the preclinical studies that are performed with actinium-225-radiopharmaceuticals for an improved understanding of their biological effects, as well as lay the foundation for wider future studies.

CRediT authorship contribution statement

Reyes L.; Giglio J; Bentura M.; Zirbesegger K. and Arredondo F contributed to draft this paper and review. Giglio J and Zirbesegger performed labeling and quality control of the radiopharmaceuticals. Dapueto R: writing, review & editing. Reyes L. and Bentura M. performed in vivo studies. Alfaya L; Arredondo F and Dapueto R. performed in vitro studies. Falasco G. and Urritia L.: data processing of in vivo studies. Duarte P. and Gambini JP. review.

Declaration of competing interest

The authors declare that they have no known competing financial interests or personal relationships that could have appeared to influence the work reported in this paper.

Acknowledgments

To the International Atomic Energy Agency (IAEA). **IAEA Research Agreement No:** 26344.

References

[1] Sung H, Ferlay J, Siegel RL, Laversanne M, Soerjomataram I, Jemal A, et al. Global cancer statistics 2020: GLOBOCAN estimates of incidence and mortality worldwide for 36 cancers in 185 countries. CA Cancer J Clin 2021;71:209–49. https://doi.org/10.3322/caac.21660.

[2] Sathekge MM, Lawal IO, Bal C, Bruchertseifer F, Ballal S, Cardaci G, et al. Actinium-225-PSMA radioligand therapy of metastatic castration-resistant prostate cancer (WARMTH act): a multicentre, retrospective study. Lancet Oncol 2024;25(2):175–83. https://doi.org/10.1016/S1470-2045(23)00638-1. Feb.

[3] Ruigrok EAM, van Weerden WM, Nonnekens J, de Jong M. The future of PSMA-targeted radionuclide therapy: an overview of recent preclinical research. Pharmaceutics 2019;11. https://doi.org/10.3390/pharmaceutics11110560.

[4] Gorges TM, Riethdorf S, von Ahsen O, Nastał YP, Röck K, Boede M, et al. Heterogeneous PSMA expression on circulating tumour cells: a potential basis for stratification and monitoring of PSMA-directed therapies in prostate cancer. Oncotarget 2016;7(23):34930–41. https://doi.org/10.18632/oncotarget.9004. Jun 7.

[5] Current K, Meyer C, Magyar CE, et al. Investigating PSMA-targeted radioligand therapy efficacy as a function of cellular PSMA levels and intratumoural PSMA heterogeneity. Clin Cancer Res 2020;26(12):2946–55. https://doi.org/10.1158/1078-0432.CCR-19-1485.

[6] Sartor Oliver, Herrmann Ken. Prostate Cancer treatment: 177Lu-PSMA-617 considerations, concepts, and limitations. J Nucl Med 2022;63:823–9. https://doi.org/10.2967/jnumed.121.262413.

[7] Chi KN, Armstrong AJ, Krause BJ, Herrmann K, Rahbar K, de Bono JS, et al. Safety analyses of the phase 3 VISION trial of [177Lu]Lu-PSMA-617 in patients with metastatic castration-resistant prostate Cancer. Eur Urol 2024;85(4):382–91. https://doi.org/10.1016/j.eururo.2023.12.004. Apr.

[8] Heck MM, Tauber R, Schwaiger S, Retz M, D'Alessandria C, Maurer T, et al. Treatment outcome, toxicity, and predictive factors for radioligand therapy with 177Lu-PSMA-I&T in metastatic castration-resistant prostate cancer. Eur Urol 2019;75(6):920–6. https://doi.org/10.1016/j.eururo.2018.11.016. Jun.

[9] Roobol SJ, van den Bent I, van Cappellen WA, Abraham TE, Paul MW, Kanaar R, et al. Comparison of high- and low-LET RadiationInduced DNA double-Strand break processing in living cells. Int J Mol Sci 2020;21. https://doi.org/10.3390/ijms21186602.

[10] Kassis AI. Therapeutic radionuclides: biophysical and radiobiologic principles. Semin Nucl Med 2008;38:358–66. https://doi.org/10.1053/j.semnuclmed.2008.05.002.

[11] Bidkar AP, Zerefa L, Yadav S, VanBrocklin HF, Flavell RR. Actinium-225 targeted alpha particle therapy for prostate cancer. Theranostics 2024;14(7):2969–92. https://doi.org/10.7150/thno.96403.

[12] Ling SW, de Blois E, Hooijman E, van der Veldt A, Brabander T. Advances in 177Lu-PSMA and 225Ac-PSMA radionuclide therapy for metastatic castration-resistant prostate Cancer. Pharmaceutics 2022;14(10):2166. https://doi.org/10.3390/pharmaceutics14102166. Oct 11.

[13] Giglio J, Zeni M, Savio E, Engler H. Synthesis of an Al(18)F radiofluorinated GLU-UREA-LYS(AHX)-HBED-CC PSMA ligand in an automated synthesis platform. EJNMMI Radiopharm Chem 2018;3:4. https://doi.org/10.1186/s41181-018-0039-y.

[14] Vichai V, Kirtikara K. Sulforhodamine B colorimetric assay for cytotoxicity screening. Nat Protoc 2006;1:1112–6. https://doi.org/10.1038/nprot.2006.179.

[15] Lee H. Relative efficacy of ^{225}Ac-PSMA-617 and ^{177}Lu-PSMA-617 in prostate cancer based on subcellular dosimetry. Mol Imaging Radionucl Ther 2022;31:1–6. https://doi.org/10.4274/mirt.galenos.2021.63308.

[16] Ruigrok EAM, Tamborino G, de Blois E, Roobol SJ, Verkaik N, De Saint-Hubert M, et al. In vitro dose effect relationships of actinium-225- and lutetium-177-labeled PSMA-I&T. Eur J Nucl Med Mol Imaging 2022;49:3627–38. https://doi.org/10.1007/s00259-022-05821-w.

[17] Afshar-Oromieh A, Avtzi E, Giesel FL, Holland-Letz T, Linhart HG, Eder M, et al. The diagnostic value of PET/CT imaging with the (68)Ga-labelled PSMA ligand HBED-CC in the diagnosis of recurrent prostate cancer. Eur J Nucl Med Mol Imaging 2015;42:197–209. https://doi.org/10.1007/s00259-014-2949-6.

[18] Benešová M, Bauder-Wüst U, Schäfer M, Klika KD, Mier W, Haberkorn U, et al. Linker modification strategies to control the prostate-specific membrane antigen (PSMA)-targeting and pharmacokinetic properties of DOTA-conjugated PSMA inhibitors. J Med Chem 2016;59:1761–75. https://doi.org/10.1021/acs.jmedchem.5b01210.

[19] Sartor O, de Bono J, Chi KN, Fizazi K, Herrmann K, Rahbar K, et al. Lutetium-177-PSMA-617 for metastatic castration-resistant prostate cancer. N Engl J Med 2021;385:1091–103. https://doi.org/10.1056/NEJMoa2107322.

[20] Kratochwil C, Bruchertseifer F, Giesel FL, Weis M, Verburg FA, Mottaghy F, et al. 225Ac-PSMA-617 for PSMATargeted α radiation therapy of metastatic castration-resistant prostate Cancer. J Nucl Med 2016;57:1941–4. https://doi.org/10.2967/jnumed.116.178673.

[21] Nelson BJB, Andersson JD, Wuest F. Targeted alpha therapy: progress in radionuclide production, radiochemistry, and applications. Pharmaceutics 2020;13(1). https://doi.org/10.3390/pharmaceutics13010049.